HHS Public Access

Selective enhancement of endothelial BMPR-II with BMP9 reverses pulmonary arterial hypertension

Lu Long[1,*], **Mark L. Ormiston**[1,*], **Xudong Yang**[1,*], **Mark Southwood**[2], **Stefan Gräf**[1], **Rajiv D. Machado**[3], **Matthias Mueller**[4], **Bernd Kinzel**[4], **Lai Ming Yung**[5], **Janine M. Wilkinson**[1], **Stephen D. Moore**[1], **Kylie M. Drake**[6], **Micheala A. Aldred**[6], **Paul Yu**[5], **Paul D. Upton**[1,#], and **Nicholas W. Morrell**[1,#]

[1]University of Cambridge, Department of Medicine, Addenbrooke's Hospital, Cambridge, UK

[2]Department of Pathology, Papworth Hospital, Papworth Everard, UK

[3]University of Lincoln, School of Life Sciences, Lincoln, UK

[4]Novartis Institute for Biomedical Research, Basel, CH

[5]Division of Cardiovascular Medicine, Department of Medicine, Brigham and Women's Hospital and Harvard Medical School, Boston, MA

[6]Genomic Medicine Institute, Lerner Research Institute, Cleveland Clinic Cleveland, OH

Abstract

Genetic evidence implicates the loss of bone morphogenetic protein type II receptor (BMPR-II) signaling in the endothelium as an initiating factor in pulmonary arterial hypertension (PAH). However, selective targeting of this signaling pathway using BMP ligands has not yet been explored as a therapeutic strategy. We identified BMP9 as the preferred ligand for preventing apoptosis and enhancing monolayer integrity in both pulmonary arterial endothelial cells and blood outgrowth endothelial cells from subjects with PAH bearing mutations in BMPR-II. In vivo, we report the spontaneous generation of PAH in a mouse model bearing a heterozygous knock-in of a human BMPR-II mutation, *R899X*. Administration of BMP9 reversed established PAH in

Corresponding Author: Nicholas W. Morrell, University of Cambridge, Department of Medicine, Level 5, Addenbrooke's Hospital, Box 157, Hills Road, Cambridge, CB2 2QQ, nwm23@cam.ac.uk, Tel.: +44 (0)1223 762007, Fax: +44 (0)1223 336846.
*These authors contributed equally to this work
#Joint senior authors

Bmpr2^{+/R899X} mice, as well as in models of disease developed in response to either monocrotaline or VEGF receptor inhibition combined with chronic hypoxia. These results demonstrate the promise of direct enhancement of endothelial BMP signaling as a novel therapeutic strategy for PAH.

Heritable and idiopathic pulmonary arterial hypertension (PAH) are characterized by narrowing and obliteration of precapillary pulmonary arteries, secondary to proliferation and apoptosis resistance of endothelial cells, smooth muscle cells, and fibroblasts[1]. The resulting increase in pulmonary vascular resistance causes severe elevation of pulmonary artery pressure, leading to right ventricular hypertrophy and ultimately death from right heart failure[2]. The identification of heterozygous germline mutations in the gene encoding the bone morphogenetic protein type II receptor (BMPR-II) in 2000[3,4] provided major insights into the pathobiology of heritable PAH. Subsequent studies also identified BMPR-II mutations in 15–40% of idiopathic PAH cases[5], and found that reduced BMPR-II expression is a feature of non-genetic forms of PAH in humans[6] and animal models[7].

Genetic evidence strongly implicates the endothelial cell as the key initiating cell type in PAH. Previous studies showed that conditional deletion of BMPR-II in the endothelium is sufficient to induce PAH in a proportion of mice[8] and that rescue of endothelial BMPR-II expression reverses experimental pulmonary hypertension[9–11]. In addition, mutations in the type I receptor, ALK-1[12], and the type I receptor accessory protein, endoglin[13], are found in individuals with PAH, both of which are almost exclusively expressed on the endothelium. Despite this evidence, the precise nature of the endothelial dysfunction in the pathobiology of PAH and the involvement of BMP signaling in this process remain uncertain. Although established PAH is characterized by the excessive clonal proliferation of pulmonary endothelial cells[14] as a component of obstructive cellular lesions, the initiation of disease pathology[15,16,17] has been linked to a paradoxical increase in endothelial cell apoptosis. Additional studies have identified a role for endothelial BMPR-II loss in the exacerbation of vascular permeability and the altered translocation of leukocytes across the vascular wall[18–20].

While *in vitro* studies using pulmonary artery smooth muscle cells (PASMCs) demonstrated that increasing concentrations of BMP ligand overcomes the loss of function associated with mutations in the BMP signaling pathway[21], to date, no study has therapeutically delivered BMP ligand *in vivo* to provide proof-of-concept for such an approach in the treatment of PAH. The complexity of the BMP receptor family, which is comprised of four type-II receptors, five type-I receptors and over twenty BMP ligands[22], may account for the absence of such studies. Identifying an appropriate ligand to selectively target the pulmonary endothelium presents a significant challenge. Recently, BMPR-II was found to form a signaling complex with ALK-1 and signal specifically in response to BMP9 and 10 in microvascular endothelial cells[23]. Unlike other BMPs, BMP9 circulates at measureable concentrations in serum and is thought to act as a vascular quiescence factor, blocking angiogenesis *in vitro*[24] and *in vivo*[25], making it a candidate for therapeutically targeting the dysfunctional pulmonary endothelium.

Here we examined the therapeutic administration of BMP9 to prevent and reverse established PAH by selectively enhancing endothelial BMPR-II signaling. BMP9 acts directly on the endothelium to promote vascular stability by preventing both apoptosis and angiogenesis, and by promoting monolayer integrity. We also report a novel mouse model of PAH, bearing a constitutive knock-in of a common human disease causing mutation at amino acid 899 (*R899X*) of the endogenous *Bmpr2* locus. Unlike previous mouse models of somatic BMPR-II haploinsufficiency[26,27], mice heterozygous for this knock-in (*Bmpr2[+/R899X]*) spontaneously develop pulmonary hypertension. The therapeutic delivery of BMP9 effectively prevents and reverses established pulmonary hypertension in both the knock-in model and the monocrotaline and sugen-hypoxia models of PAH. Together, these studies underscore a role for BMP9 as a vascular stability and quiescence factor and provide a translational framework for the delivery of this BMP ligand as a treatment strategy for PAH.

Results

BMP9 elicits endothelial-selective transcriptional regulation

We sought to identify a BMP ligand for therapeutic delivery that would selectively and efficiently enhance canonical BMP signaling in the endothelium while minimizing the potential for deleterious off-target effects, such as the calcification of soft tissue[28]. As an initial screen, we stimulated human pulmonary arterial endothelial cells (PAECs) with BMP9, BMP2 or BMP6 and assessed changes in gene transcription by microarray. Unlike BMP2 and BMP6, which induced negligible gene expression, BMP9 induced the differential regulation of 1883 genes (adjusted P value < 0.05), including several key components of canonical BMP signaling such as *ID1*, *ID2* and *BMPR2* (Fig. 1a–c). Generally applicable gene-set enrichment (GAGE) analysis for common signaling pathways and cellular processes revealed TGF-β signaling as the only pathway to be significantly (P=0.0012) upregulated by BMP9. However, BMP9 also downregulated other pathways, including apoptotic cell signaling (Fig. 1d; Supplementary Fig. 1). Signaling pathway impact analysis (SPIA) of common signaling pathways confirmed the TGF-β pathway as the only pathway to be enhanced in response to BMP9 treatment, supporting a central role for the canonical Smad pathway in the actions of BMP9 (Fig. 1e). We obtained similar results using blood outgrowth endothelial cells (BOECs) from healthy subjects, which, like PAECs, responded almost exclusively to BMP9 stimulation (Supplementary Fig. 2). Analysis of BMP9-induced gene expression for specific members of the TGF-β pathway revealed an enhancement of classical downstream targets of BMP signaling, whereas expression levels of TGF-β$_1$ downstream targets, including PAI-1, Myc and CTGF, remained unchanged (Supplementary Fig. 3a). Of note, BMP9 did not alter the expression of a selected group of endothelial-derived paracrine factors and typical PASMC mitogens, including members of the PDGF and FGF families of cytokines (Supplementary Fig. 3b).

Validation of BMP responsiveness in PAECs by immunoblotting confirmed robust induction of Smad1/5/8 phosphorylation, ID1 and ID3 in PAECs in response to BMP9 concentrations as low as 0.1 ng/mL. In contrast, other BMPs were much less effective over the range of doses tested (Fig. 1f, Supplementary Fig. 4b). As a further measure of

endothelial selectivity, PASMCs displayed a modest response to BMP9 when compared to an equivalent dose range of other BMPs (Supplementary Fig. 4a, b). We observed similar responses in additional endothelial cell lines (Supplementary Fig. 4b). As a further measure of the endothelial selectivity of BMP9 in the pulmonary circulation, we stimulated freshly isolated rat pulmonary arteries *ex vivo* with BMP9 and assessed for induction of Smad1/5 phosphorylation. We observed phospho-Smad immunostaining exclusively in the endothelium, with no measurable signal in the underlying smooth muscle (Supplementary Fig. 4c).

The array study also identified a notable capacity of BMP9 to induce *BMPR2* gene expression, which was validated by immunoblotting and qPCR (Fig. 1f–g). siRNA knockdown of *Smad1*, with or without *Smad5* knockdown, eliminated the capacity of BMP9 to enhance *BMPR2* expression (Supplementary Fig. 5a–d), supporting the importance of canonical Smad signaling to this process. To confirm this finding, we identified a putative Smad binding site on the *BMPR2* promoter (Supplementary Fig. 5e) and used chromatin immunoprecipitation in human microvascular endothelial cells (HMEC-1) to demonstrate p-Smad1/5 and Smad4 binding to this region, which was lost following siRNA knockdown of *Smad1* and enhanced in response to treatment with BMP9 (Fig. 1h). HMEC-1 cells transfected with a luciferase reporter construct downstream of a 5kb segment of the *BMPR2* promoter exhibited enhanced basal luciferase activity versus a control vector without the *BMPR2* promoter region, which was further elevated in response to BMP9 treatment (Fig. 1i). Mutation of the putative Smad binding region in the 5kb segment reduced both baseline luciferase activity and BMP9 regulation of the promoter. We did not observe a similar enhancement of *BMPR2* expression in PASMCs in response to treatment with BMP9, BMP2 or BMP6 (Supplementary Fig. 5f).

BMP9 prevents endothelial cell apoptosis and permeability

As reported previously[29], PAECs stimulated with TNFα in the presence of cyclohexamide exhibited elevated JNK phosphorylation as a part of an apoptotic signaling cascade (Fig. 2a). Pre-treatment of PAECs with BMP9 prevented JNK phosphorylation and blocked the induction of apoptosis, as demonstrated by immunoblotting for cleaved caspase-3 (Fig. 2b) and by flow cytometry for early apoptotic, Annexin-V+/PI− cells (Fig. 2c, d). Since BMP9 signals via complexes of the type I receptor ALK1 with either BMPR-II or ActR-II as the type II receptor[30], we determined whether the anti-apoptotic effects of BMP9 were indeed BMPR-II dependent. siRNA knockdown of BMPR-II (Fig. 2e) eliminated the capacity of BMP9 to prevent apoptosis when compared to controls (Fig. 2f, g). Importantly, siRNA knockdown of *Smad1* and *Smad5* also partially blocked the anti-apoptotic effect of BMP9, reinforcing the importance of canonical Smad signaling in this process (Supplementary Fig. 6).

BOECs from healthy controls and individuals with PAH-associated mutations in *BMPR2* were used as a surrogate for PAECs to determine the efficacy of BMP9 therapy in the context of *BMPR2* mutations. Although mutation-bearing BOECs displayed an increased susceptibility to apoptosis when compared to cells isolated from healthy control subjects (Fig. 3a), BMP9 blocked JNK phosphorylation (Fig. 3b) and apoptosis in both control and

mutation-bearing BOECs (Fig. 3a, c), supporting the benefit of this approach, even in the context of BMPR-II deficiency.

We also examined the effect of BMP9 on endothelial barrier integrity (Fig. 3d–g). LPS stimulation of control BOECs resulted in increased monolayer permeability that was blocked by the addition of BMP9. BOECs with *BMPR2* mutations demonstrated greater permeability in response to LPS. However, as with the apoptotic responses, heterozygous *BMPR2* mutation in these cells did not prevent the capacity of BMP9 to block LPS-induced monolayer permeability. BMP9 also reduced the basal permeability of unstimulated, mutation bearing BOECs (Fig. 3f). We observed similar results in PAECs in response to TNFα or thrombin-induced permeability (Supplementary Fig. 7a). VE-cadherin staining demonstrated impaired cell-cell junctions in response to all three stimuli that was blocked by BMP9 (Fig. 3g, Supplementary Fig. 7b).

Bmpr2[+/R899X] mice develop age-related pulmonary hypertension

In order to determine whether exogenous administration of BMP9 would be beneficial in a mouse model of PAH that mimics the genetics of human disease, we created a knock-in mouse, bearing the human disease-associated *R899X* premature stop mutation in exon 12 of the endogenous *Bmpr2* locus (Supplementary Fig. 8a). As reported for *Bmpr2* null mice[31], mice homozygous for the *R899X* mutation were non-viable. Heterozygous *Bmpr2[+/R899X]* mice developed normally and displayed reduced BMPR-II protein (Supplementary Fig. 8b) and mRNA (Supplementary Fig. 8c), consistent with an *R899X* mutation that leads to mRNA degradation by nonsense mediated mRNA decay (NMD) in humans[32]. We confirmed NMD of the *R899X* transcript in both mouse and human smooth muscle cells bearing the mutant allele (Supplementary Fig. 8d–i). *Bmpr2[+/R899X]* mice exhibited normal right ventricular systolic pressures (RVSP) at 3 months of age (Supplementary Fig. 9a), but developed elevated RVSP by 6 months (Fig. 4a). While this increase in RVSP was not accompanied by right ventricular hypertrophy (Fig. 4b), 6 month-old *Bmpr2[+/R899X]* mice did exhibit enhanced muscularization of peripheral pulmonary arteries in the lung (Fig. 4c, d). Further characterization of left ventricular function demonstrated no significant differences in left ventricular end diastolic pressure or cardiac output between 6 month-old *Bmpr2[+/R899X]* and WT controls (Supplementary Table 1). In contrast, 6 month-old *Bmpr2^{+/−}* mice did not exhibit elevated RVSP or RV hypertrophy in our hands (Supplementary Fig. 9e–f).

To examine the importance of canonical Smad signaling in this PAH model, we also assessed the pulmonary vascular phenotype of mice heterozygous for *Smad1*[33]. Male *Smad1^{+/−}* mice did not exhibit raised RVSP or RV hypertrophy at 3 or 6 months (Fig. 4e, f; Supplementary Fig. 9b–d). However, the generation of *Bmpr2[+/R899X]/Smad1^{+/−}* compound heterozygotes resulted in mice that, by 6 months, developed more severe elevations in RVSP than those heterozygous for *R899X* alone (Fig. 4e). Unlike *Bmpr2[+/R899X]* mice, this more pronounced elevation in RVSP was also accompanied by right ventricular hypertrophy in *Bmpr2[+/R899X]/Smad1^{+/−}* mice when compared to WT controls (Fig. 4F). Both *Bmpr2[+/R899X]* and *Bmpr2[+/R899X]/Smad1^{+/−}* compound heterozygous mice exhibited

reduced BMPR-II protein and pulmonary Smad1/5 phosphorylation compared to WT littermate controls (Supplementary Fig. 9e–g).

BMP9 reverses pulmonary hypertension in Bmpr2$^{+/R899X}$ mice

Treatment of 6 month-old *Bmpr2$^{+/R899X}$* mice with BMP9 (75 ng daily, i.p.) for 4 weeks reversed all indices of PAH in this chronic disease model, returning RVSP to the level seen in WT mice (Fig. 4a) and reversing the enhanced pulmonary arterial muscularization in these mice (Fig. 4c, d). The dose selection was based on an initial, 7-day chronic dose-ranging study in rats (Supplementary Fig. 10a) and translated to mice on a weight/weight basis (Supplementary Fig. 10b).

We also used pulmonary endothelial cells from WT and *Bmpr2$^{+/R899X}$* mice to assess the capacity of BMP9 to enhance monolayer integrity *in vitro*. As with *BMPR2* mutation-bearing BOECs, endothelial monolayers from *Bmpr2$^{+/R899X}$* mice displayed increased permeability both at baseline and following LPS stimulation. BMP9 prevented LPS-induced permeability in endothelial monolayers from both WT and *Bmpr2$^{+/R899X}$* mice (Fig. 4g; Supplementary Fig. 10c, d). *In vivo, Bmpr2$^{+/R899X}$* and WT mice injected with LPS developed pulmonary vascular leak, quantified by extravasation of Evans blue dye into lung tissue (Fig. 4h). *Bmpr2$^{+/R899X}$* mice demonstrated increased dye extravasation compared to WT littermates, which was blocked with BMP9 to a similar degree in both groups (Fig. 4i).

To further exclude the possibility that BMP9 was acting through a direct effect on smooth muscle, we isolated PASMCs from WT and *Bmpr2$^{+/R899X}$* mice. While BMP4 reduced PASMC proliferation, BMP9 had no effect (Supplementary Fig. 10e, f).

BMP9 reverses monocrotaline-induced pulmonary hypertension

We assessed the efficacy of BMP9 treatment in the monocrotaline rat model of PAH, a non-genetic model of disease in which reduction of BMPR-II expression is a central feature[7,34]. BMP9 treatment for 21 days (600 ng/day, i.p.) immediately following exposure to monocrotaline prevented elevation of RVSP, right ventricular hypertrophy and pulmonary arterial muscularization (Fig. 5a–d). In a protocol where BMP9 dosing was commenced 3 weeks after monocrotaline, in the presence of the established PAH, two weeks of daily BMP9 treatment inhibited the progression of PAH (Fig. 5c–f). In agreement with our previous reports, rats treated with monocrotaline displayed reduced lung BMPR-II protein levels and impaired canonical BMP signaling (Supplementary Fig. 11a–d). Treatment with BMP9 from days 0 to 21 restored BMPR-II levels and downstream signaling to near normal levels.

Endothelial apoptosis is believed to be a primary factor in the initiation of PAH models[16,17] and human disease[15]. Staining of lung tissue for cleaved caspase-3 not only revealed enhanced pulmonary endothelial cell apoptosis at five days post-monocrotaline, but also in established disease at three weeks post-monocrotaline (Fig. 5g, h). Daily administration of BMP9 prevented enhanced apoptosis at both time points. Immunoblotting of whole lung lysates confirmed a reduction in total cleaved caspase-3 in response to BMP9 at both three and five weeks post-monocrotaline (Supplementary Fig. 11e).

BMP9 reverses Sugen-hypoxia induced pulmonary hypertension

We also examined the efficacy of BMP9 in the more severe PAH model of rats exposed to chronic hypoxia in combination with the VEGF receptor blocker SU-5416[17] (Fig. 6a). Rats given SU-5416 and exposed to three weeks of hypoxia (10% O_2) and an additional 5 weeks of normoxia developed severe pulmonary hypertension and right ventricular hypertrophy (Fig. 6b–c) as well as extensive pulmonary arterial muscularization (Fig. 6d–e). Daily BMP9 (600 ng/day, i.p.) from weeks 8 to 11 resulted in a reversal of established disease, including a reduction in RVSP, RV hypertrophy and vascular remodeling when compared to saline-treated controls (Fig. 6b–e).

Established disease was also accompanied by the concurrent formation of both angio-obliterative lesions (Fig. 6f, h) and heightened endothelial cell apoptosis (Fig. 6g), as well as reduced Smad1/5 phosphorylation (Supplementary Fig. 12a–b), all of which were reversed by BMP9. Immunoblotting of whole lung lysates for cleaved caspase-3 and PCNA further supported the capacity of BMP9 to simultaneously prevent excessive endothelial cell apoptosis and pathological angiogenesis in this model (Supplementary Fig. 12a). While BMP9 did not reverse elevated VEGFA gene expression in the lungs of rats treated with SU-5416 and hypoxia, it did block VEGF-induced endothelial cell proliferation and tube formation *in vitro* (Supplementary Fig. 12c–i). Assessment of LV function revealed no significant changes in cardiac output in diseased animals given BMP9 or saline when compared to healthy controls (Supplementary Table 1).

Similarly, mice given SU-5416 and exposed to three weeks of hypoxia (10% O_2) developed moderate-to-severe pulmonary hypertension and right ventricular hypertrophy, accompanied by increased pulmonary arteriolar muscularization (Supplementary Fig. 13a–c). Administration of BMP9 (75 ng/day, i.p.) throughout the period of treatment with SU-5416 and hypoxia resulted in normalization of right ventricular systolic pressure and right ventricular mass, and abrogated the muscularization of small arterioles. Treatment of mice with BMP9 did not result in heterotopic ossification at the sites of i.p. injection, based on x-ray and micro-CT analysis (Supplementary Fig. 13d). Moreover, daily intramuscular injection of mice with BMP9 (75 ng/day) for 3 weeks failed to elicit intramuscular heterotopic ossification (Supplementary Fig. 13e).

Discussion

We report the first use of a BMP ligand to target and enhance endothelial BMPR-II signaling and reverse established PAH in animal models of disease. This work is also the first to show that mice heterozygous for a human disease causing mutation are susceptible to PAH, providing a new genetic model for this disease that, unlike previous models, closely mimics the human genetics of PAH.

One challenge associated with therapeutic application of BMPs for the treatment of PAH is the identification of a ligand that preferentially targets the pulmonary endothelium. Our array screen of PAECs treated with different BMP ligands demonstrated the superiority of BMP9 for stimulating the pulmonary endothelium. Of note is our observation that BMP2, 4 and 6 possess minimal ability to stimulate PAECs, which at first sight contrasts with other

previously published findings. This discrepancy can be largely accounted for by differences in the concentrations of BMPs used. The majority of papers describing a response of endothelial cells to BMP2, 4 or 6 used concentrations in excess of 10ng/ml and often use a range of 50–200 ng/ml[15,35]. Here we show the response of PAECs to BMP9 is already maximal at 1 ng/ml. These findings demonstrate that other BMPs may be used to stimulate the endothelium, but only at high doses that will have no selectivity for the endothelium and likely promote heterotopic ossification. In contrast, BMP9 allows for selective stimulation of canonical BMP signalling in pulmonary endothelial cells at concentrations that do not induce signaling in PASMCs and do not promote ossification. As ALK1 is also expressed in hepatocytes, mesenchymal cells, chondrocytes and cardiomyocytes, we cannot categorically exclude non-endothelial mechanisms of BMP9 treatment.

In vitro and *in vivo* studies confirmed the capacity of BMP9 to block apoptosis and enhance vascular stability, two pathways critically dysregulated in the pathogenesis of PAH[15–20]. The ability of BMP9 to prevent endothelial apoptosis *in vitro* is in agreement with previous studies that reported the anti-apoptotic effect of various BMP ligands[15,36]. Despite the fact that this action of BMP9 is dependent on BMPR-II, we were able to show that BMP9 provides protection in *BMPR2* mutation-bearing BOECs, presumably due to increased ligand interaction and signaling via the wild type receptor. We demonstrate that BMP9 inhibited endothelial permeability induced by a variety of agents relevant to PAH. Endothelial permeability is increasingly implicated in PAH pathobiology and a recent study identified that loss of BMPR-II promotes SRC-dependent caveolar trafficking defects in heritable PAH as a potential mechanism[37].

Beyond the direct effects of BMP9 on endothelial cell function, we demonstrate the capacity of BMP9 to increase BMPR-II levels via a Smad-binding region on the *BMPR2* promoter. In canonical BMP signaling, interactions of ligands with heterodimers of type I and type II receptors leads to phosphorylation of a restricted set of receptor activated Smad proteins (Smads 1,5 and 8). However, non-Smad mediated BMP signaling is involved in certain cellular responses. Despite the recent identification of rare mutations in *Smad1* and *Smad8* in individuals with PAH[38,39], the relative contribution of Smad and non-Smad mediated signaling to the pathobiology of PAH remains uncertain. Our observation that compound heterozygous mice, bearing loss-of-function mutations in both *Bmpr2* and *Smad1*, develop more severe spontaneous PAH than that observed in mice heterozygous for *Bmpr2* alone supports a central role for the canonical BMPR-II/Smad signaling pathway in PAH. This is supported by a previous study showing that conditional deletion of *Smad1* in endothelial cells in mice promotes the development of PAH[40].

Our report of the spontaneous development of PAH in the *Bmpr2+/R899X* knock-in mouse is a major development, which for the first time provides an experimental model of disease that closely mimics the human genetics of PAH, leading to NMD of the mutant transcript. Although *Bmpr2+/R899X* mice spontaneously develop elevated right ventricular systolic pressures and enhanced pulmonary arteriolar muscularization at 6 months of age, these changes were not accompanied by right ventricular hypertrophy. One possibility is that the modest increase in RVSP in these mice (~35mmHg) was not sufficient to induce measurable RV hypertrophy. This possibility is supported by the fact that compound *Bmpr2+/R899X/*

Smad1^{+/−} heterozygotes did develop RV hypertrophy in response to a more severe elevation of RVSP. Alternatively, a recent reports in a pulmonary arterial banding model of RV hypertrophy showed that the transgenic expression of a stabilized form of mutant *Bmpr2-R899X* in the heart results in reduced RV remodeling associated with intra-cardiomyocyte lipid deposition[41]. It is noteworthy that aged *Bmpr2*^{+/R899X} mice are susceptible to PAH, whereas *Bmpr2* heterozygous null mice are not. There is no clear explanation for this observation, since both would be expected to result in haploinsufficiency. It remains possible that incomplete NMD of the mutant transcript in *Bmpr2*^{+/R899X} mice plays a role, although we found no evidence for this.

The finding that BMP9 treatment reverses established disease in three animal models of PAH is critical, as any viable treatment will need to be effective in a patient population that typically presents with advanced disease. The capacity of BMP9 to reverse disease in the Sugen-hypoxia model is a particularly important indicator of the clinical suitability of this treatment strategy, as it is the only model to recapitulate the intimal lesions and advanced vascular remodeling observed in individuals with PAH. In these models, we have shown that, as in our cultured endothelial cells, BMP9 promotes vascular stability by simultaneously preventing apoptosis and blocking pathological angioproliferation. Our observation of increased endothelial apoptosis at later time points in both the monocrotaline and Sugen-hypoxia rat models support the suggestion that endothelial apoptosis is not only a driving factor in disease onset, but an ongoing phenomenon in established disease, occuring concurrently with pathological angioproliferation. This finding is supported by our observation that *BMPR2* mutation-bearing BOECs are more susceptible to apoptotic stimuli even when isolated from individuals with established PAH.

In conclusion, our work provides proof-of-concept for the treatment of PAH through the direct enhancement of endothelial BMPR-II signaling with BMP9. BMP9 not only protects pulmonary arterial endothelial cells from apoptosis and promotes vascular stability, but also increases *BMPR2* gene expression, allowing for further enhancement of BMPR-II signaling. These effects were still observed in cells derived from individuals bearing mutations in *BMPR2*, suggesting that this treatment might be efficacious in PAH patients with or without a mutation. Taken together, our findings suggest that approaches based on targeting the canonical endothelial BMPR-II/ALK1 complex using recombinant ligands or small molecule receptor agonists may provide a promising new approach for the treatment of PAH.

Online Methods

Cell Culture

Human ECs were purchased from Lonza (Basel, Switzerland). PAECs, HUVECs, HAECs and HMEC-1 cells were cultured in EGM-2 with 2% FBS (Lonza), as per supplier's instructions. Human BOECs were generated from 40–80 mL peripheral blood, as described previously[42]. BOECs were cultured in EGM-2MV with 10% standard grade FBS (Life Technologies, Carlsbad, CA) and were used for experiments between passages 4 and 8. Unless specified otherwise, treatment of human endothelial cells with BMPs was performed in EBM-2 (Lonza) with 0.1% FBS.

The endothelial nature of BOECs was assessed by flow cytometry for endothelial surface marker expression as described previously[42]. All cell lines were routinely tested for mycoplasma contamination. For BOEC generation, all blood donors provided informed consent in accordance with human study 07/H0306/134 (Cambridgeshire 3 Research Ethics Committee). Information on the specific *BMPR2* mutations present in BOECs is specified in Supplementary Table 2.

Mouse lung microvascular endothelial cells were isolated as described previously[43] with minor modifications. Briefly, minced lung tissue was digested for 30 minutes at 37°C in 2mg/mL Collagenase I (Sigma Aldrich, St. Louis, MO), dissolved in DPBS with calcium and magnesium and filtered through a 70μm cell strainer. The resultant cell suspension was incubated for 10 minutes at room temperature with sheep anti-rat IgG Dynabeads (Life Technologies), pre-conjugated with rat anti-mouse PECAM-1 (BD-Pharmingen, Franklin Lakes, NJ). Magnetically isolated cells were washed multiple times DMEM and plated on tissue culture plates pre-coated with 0.1% gelatin (Sigma) for 24 hours in Endothelial Growth Medium, consisting of DMEM with 20% FBS, 1x Penicillin-Streptomycin-Glutamine (Life Technologies), 0.1mg/mL heparin (Sigma) and 0.1mg/mL Endothelial Cell Growth Factor (Biomed Tech Inc, Ward Hill, MA). After 24 hours, cultures were washed to remove non-adherent cells and allowed to grow for 5–9 days until near confluent. Cells were then trypsinized and endothelial cells were purified by a second round of positive magnetic selection with Dynabeads. Resultant endothelial cells, which grow with a typical cobblestone morphology, were then re-plated on gelatin coated plates in Endothelial Growth Medium.

Human and mouse PASMCs were isolated and cultured as described previously.[44] Unless specified otherwise, tretament of PASMCs with BMPs was performed in DMEM with 0.1% FBS.

Microarray

PAECs (n=4) or BOECs (n=3) from healthy subjects were quiesced in M199 media with 0.1% FBS for 12 hours prior to a 4 hour stimulation in new media with vehicle, 1 ng/mL BMP9, 10 ng/mL BMP2 or 10 ng/mL BMP6 (all from R&D Systems, Minneapolis, MN). Cell monolayers were lysed in Trizol and purified mRNA was hybridized to Human Genome U133 Plus 2.0 GeneChips (Affymetrix, Santa Clara, CA). Quality control, background correction and normalization were performed using R/Bioconductor (http://bioconductor.org). Differential gene expression was assessed by fitting linear models and resulting p-values were adjusted for multiple testing[45]. Enrichment of gene-sets was determined using Generally Applicable Gene-set Enrichment (GAGE)[46] and Signaling Pathway Impact Analysis (SPIA)[47]. Pathway diagrams were generated with the pathviews package[48]. The pathway maps of interest, i.e. "Environmental Information Processing" and "Cellular Processes" were retrieved from the Kyoto Encyclopedia of Genes and Genomes (KEGG) database. Microarray data are available in the ArrayExpress database (www.ebi.ac.uk/arrayexpress) under accession number E-MTAB-2495.

siRNA knockdown and qPCR

Cells were maintained in Optimem serum free medium (Life Technologies) for 3 hours prior to the addition of Dharmafect 1 transfection reagent with or without siRNAs for *Smad1*, *Smad5* or *BMPR2* or a control pool of oligonucleotides (all Thermo Fisher, Waltham, MA) for 4 hours. After siRNA treatment, cells were returned to culture media for 24 hours prior to use. qPCR for *Smad1*, *Smad5, BMPR2* or *VEGFA* mRNA was performed as described previously[30] and presented relative to *GAPDH, β-2 microglobulin, HPRT, β-actin*, or a combination of these housekeeping genes.

Western Blotting

After the indicated duration of treatment, cells were lysed in phosphate buffered saline (PBS) containing 50mM Tris pH 8.0, 1% igepal, 0.1% SDS, 0.5% sodium deoxycholate and Roche complete protease inhibitor cocktail (Roche, Basel, Switzerland). Lysates were sonicated and frozen at −80°C until used. Cell lysates (20–40μg total protein) were separated on reducing SDS-PAGE gels and proteins were transferred to polyvinylidene fluoride membranes by semi-dry blotting. Membranes were then blocked and probed with rabbit polyclonal antibodies towards JNK (catalogue # 9252), phospho-JNK (catalogue # 9251), Smad1 (catalogue # 9743), phospho-Smad1/5/8 (catalogue # 9511, all Cell Signaling Technology, Danvers, MA) or PCNA (catalogue # ab18197, Abcam, Cambridge, UK), rabbit monoclonal antibodies towards Caspase-3 (clone 8G10), cleaved Caspase-3 (clone 5A1E), phosphorylated Smad1/5 (clone 41D10, all Cell Signaling Technology, Danvers, MA), Smad5 (clone EP619Y, Epitomics, Burlingame, CA), Id1 (clone 195-14) or Id3 (clone 17-3, both CalBioreagents, San Mateo, CA) or a mouse monoclonal antibody towards BMPR-II (clone 18/BMPR-II, BD Transduction Laboratories, Franklin Lakes, NJ). As a loading control, all blots were re-probed with a monoclonal antibody towards either α-tubulin (clone DM1A) or β-actin (clone AC-15, Sigma). Densitometry was performed using ImageJ software.

Chromatin Immunoprecipitation (ChIP) Assay

ChIP assays were performed using a chromatin immunoprecipitation assay kit (Millipore, Billerica, MA) in accordance with the manufacturer's instructions. HMEC-1 cells at 80–90% confluency were assayed either at baseline, 72 hours after siRNA knockdown of Smad1 or following a 24 hour stimulation with 1 ng/mL BMP9. Cells were cross-linked with 1% formaldehyde for 10 minutes at 37°C. 125mM glycine was added to block cross-linking. Cells were then rinsed with PBS and lysed in 200μl buffer containing 1ug/ml aprotinin, pepstatin, and 1mM phenylmethylsulfonul fluoride. Chromatin samples were sonicated with 4 sets of 10-second pulses on wet ice using a Cole Parmer, High Intensity Ultrasonic Processor/Sonicater, 50-watt model equipped with a 2mm tip and set to 30% maximum power to reduce the DNA length to 200–1000bp. The sonicated lysate was then diluted to 2ml with dilution buffer containing a protease inhibitor cocktail. After preclearing with salmon sperm DNA/Protein A-agarose for 1h at 4°C, 20μl (1%) of this solution was removed for later PCR analysis (input). 2μg of the immunoprecipitating antibodies towards C-terminal phospho-Smad1/5 or Smad4 (catalogue # 9515, Cell Signaling Technology) were added to the remaining sample (for the negative control, rabbit polyclonal IgG was added),

and the sonicated lysates were incubated overnight at 4°C. Immune complexes were collected with 60μl of salmon sperm DNA/Protein A-agarose (1h at 4°C), and agarose beads were washed with solutions of increasing ionic strength. After a final wash, bound immune complexes were eluted in a freshly prepared solution of 1% SDS, 0.1M NaHCO$_3$, and cross-links were reversed in the samples (and the input from the sonicated lysates) by heating at 65°C overnight. Samples were then treated with Proteinase K, and DNA was phenol/chloroform-extracted and precipitated. DNA was resuspended in 20μl H$_2$O, and 1μl was used for detection of the *BMPR2* promoter by PCR using the oligonucleotides 5′-GAACACATCAAAGGGGTGGT-3′ and 5′-GTGGCCTTTCTCCTTCACAC-3′, which together amplify 350bp spanning from −1797 to −1448 of the promoter region. DNA from the input was resuspended in 20μl, and 1μl was used for PCR.

BMPR2 Promoter Constructs

A 5kb fragment of the human *BMPR2* promoter was generated by polymerase chain reaction (PCR) from BAC clone RP11-68606. A 5′ primer (5′-GCG CGA GCT CTA GTC CTC CCT GCC CCT TAT-3′), including a Sac I site for subcloning, and a 3′ primer (5′-GCG CAA GCT TAG CAG GAT GGT CCA TGG TAG-3′) initiating 59bp upstream of the transcription start site and containing a Hind III site, were used. The amplified product was purified and cloned into the Sac I/Hind III-digested promoter-deficient reporter vector pGL3-basic (Promega, Madison, WI) to give the *BMPR2*-luc construct. The putative Smad binding site on the *BMPR2* promoter was mutated using the PCR-based QuickChange Site-Directed Mutagenesis kit (Stratagene, La Jolla, CA) and the following primers Fwd: 5′-GCTCTGCACCACAGGCTAGA**GGtgAtcCAG**GGCCGGGAAGAG-3′; Rev: 5′-CTCTTCCCGGCC**CTGgaTcaCT**CTAGCCTGTGGTGCAGAGC-3′, with the binding site indicated in bold and the desired point mutations indicated in lowercase. PCR products were digested with Dpn I to elimate parental DNA. Recombinant DNA was verified by sequencing.

Transfection of HMEC-1 cells

HMEC-1 cells were seeded onto 24-well plates at a density of 8×10^4 cells per well 24 hours before transfection. The transfection was performed with LipofectAMINE^{2000} reagent (Invitrogen, UK). Typically 1μg of plasmid DNA was mixed with 2μl of LipofectAMINE^{2000}. Fresh culture medium was changed 24h after transfection. 48 hours post-transfection, cells were washed with PBS and lysed. Nuclear-free supernatants were analysed for luciferase reporter gene activity (Roche Molecular Biochemicals, Germany) and corrected for protein content.

Induction of and assessment of apoptosis by Annexin-V and Propidium Iodide staining

Sixteen hours prior to the addition of an apoptotic stimulus, PAECs or BOECs were transferred into EBM-2 basal media (Lonza) with 2% FBS, 100 U/mL penicillin, 100 mg/mL streptomycin and 0.25 mg/mL amphotericin B, but without any growth factor supplements. During this incubation, cells were maintained with or without 5 ng/mL BMP9 for indicated period. Following the 16-hour incubation, cells were either left unstimulated or treated for 3 or 6 hours with 10 ng/ml TNFα and 20 μg/mL cyclohexamide to induce

apoptosis. For measurement of total and phospho-JNK, cells were lysed after 3 hours and lysates were assessed by immunoblotting. For assessment of apoptosis, cells were incubated for 6 hours after the apoptotic stimulus and either lysed for the assessment of cleaved caspase-3 by immunoblotting or trypsinized, stained with FITC-conjugated annexin-V and propidium iodide (PI, BD Biosciences) as per manufacturer's instructions and assessed by flow cytometry. Apoptotic cells were considered to be positive for annexin-V and negative for PI.

Assessment of endothelial monolayer permeability

Monolayer permeability was assessed as described previously[49]. Briefly, transwell inserts (Corning, Corning, NY) were coated for 1 hour at 37°C with 0.1 mg/mL bovine skin collagen (Sigma), washed with water 2 times and rinsed with medium prior to plating cells. Cells (4×10^5 in 100 µl complete EGM-2 medium) were plated in the top chamber and 700 µl of medium was added to the bottom chamber 24 hours prior to the addition of fresh medium to both chambers, with or without 10 or 20 ng/mL BMP9 in the upper chamber (as indicated). After 30 minutes, 25 nM horseradish peroxidase was added to the top chamber, with or without 0.4ug/ml LPS (Sigma), 1U/mL thrombin (Sigma) or 50 ng/mL TNFα (R&D Systems). Medium (20µl) was collected from the lower chamber every 30 minutes for 2 hours. HRP content of the media samples was determined by measuring absorbance after the addition of 150µl of o-Phenylenediamine dihydrochloride buffer to each well of a 96-well plate.

For VE-cadherin assays, PAECs were cultured in EBM-2 media (Lonza) with 2% FBS for 24 hours with or without LPS, thrombin, TNFα and/or 10 ng/mL BMP9. Cells were then stained with FITC-conjugated rabbit polyclonal anti-VE-cadherin (cat #: LS-C40121, 1:100, Lifespan Biosciences, Seattle, WA).

Cell Proliferation assays

For assessment of PAEC proliferation, cells were seeded at 30000 cells/well in 24-well plates and left to adhere overnight. Cells were the washed with EBM2 containing 0.1% FBS and then serum-restricted in EBM-2 containing 0.1% FBS. Cells were then treated with BMP9 (5ng/ml), $VEGF_{165}$ (30ng/ml, both R&D Systems) or both ligands combined in EBM2 containing 2% FBS and treatments were replenished after 48 hours. After 72 hours of ligand exposure, cells were trypsinised and counted using trypan blue exclusion to assess cell viability.

Proliferation of mouse PASMCs was determined as described previously[44], in the presence of 1 ng/mL BMP9 or 10 ng/mL BMP4.

Endothelial tube formation assays

PAECs were cultured in a collagen and fibronectin gel matrix as previously described[50]. Briefly, cells were combined with the gel at a final concentration of 1×10^6. The suspension was then pipetted into an angiogenesis µ-slide (Ibidi, Germany) in a volume of 10 µl/well. After 10 minutes at 37°C to allow polymerization, the gel was overlaid with 40µl of media (EBM-2, Lonza and 2% FBS), with or without 5 ng/ml BMP9 or 30 ng/mL $VEGF_{165}$ (both

R&D Systems) individually or combined. The 3-D cultures were left at 37°C for 24 hours and tube formation confirmed by brightfield microscopy. Images were collected and parameters measured and quantified using Image J software. In order to gain confocal images, gels were first fixed in 4% PFA, washed in PBS and incubated with Rhodamine labelled ULEX Europaeus Agglutinin1 (Vector Laboratories, Burlingame, CA) overnight at 4°C. After 3× 10 minute PBS washes, nuclear staining was carried out using 10µl of VectorSHIELD mounting media with DAPI (Vector Laboratories) for 30 minutes. A final x3 wash in PBS was completed.

Rodent models of PAH

For all animal work, group sizes were determined using estimates of variance and minimum detectable differences between groups that were based on our past experience with rodent models of PAH. Animals were randomized using an assigned animal identification number, allowing investigators performing all cardiopulmonary phenotyping procedures and histological analyses to be blinded to animal genotype and treatment group. All animal work was carried out in accordance with the UK Animals (Scientific Procedures) Act 1986 and approved under Home Office Project Licence 80/2460.

Mice

All mice used in this work possessed a C57Bl/6 background. $Smad1^{+/-}$ mice were obtained as a generous gift from the late Dr Anita Roberts[33]. For $Bmpr2^{+/R899X}$ mice, both male and female mice were studied. For $Smad1^{+/-}$ mice and $Smad1^{+/-}/Bmpr2^{+/R899X}$ compound heterozygotes, as well as littermate controls, only male mice were examined.

Creation of Bmpr2$^{+/R899X}$ mice

A gene targeting vector was created containing a 4.69kb 5′ homology arm and a 1.84kb 3′ homology arm, separated by a loxP flanked neomycin expression cassette (Supplementary Fig. 8). The 5′ homology arm, consisting of 4.69kb of intron 11, exon 12 and 30 bp of intron 12, was cloned into the pNTFLOX (kind gift of Dr. Jim Hughes) vector between the XhoI and NotI restriction sites using the following primers Fwd: 5′-GATC CTCGAG GTAAGGTCCT GAGGGGTTTG-3′; Rev: 5′-GATCGCGGCCGCCAAAGGGTACTGCATAACCCCT-3′. The 1.84kb 3′ homology arm, consisting of intron 12 and exon 13, was cloned into PacI and KpnI sites using the following primers: Fwd: 5′-GATCTTAATTAAGGACAGTTAA ATAAAATAGA-3; Rev: 5′-GATCGGTACCTCACAGACAATTCATTCCTA-3′. The *R899X* substitution mutation was introduced into exon 12, 200bp upstream of the 3′ end of the 5′ homology arm using the Stratagene Quickchange site-directed mutagenesis kit and the following primers: Fwd: 5′-CCATTAGAAGGTGGC**TG**AACAAATTCCAAT-3′; Rev: 5′-ATTGGAATTTGTT**CA**GCCACCTTCTAATGG-3′ following manufacturer's instructions. For homologous recombination, the 5′ homology arm was truncated to 1.72 kb and the resulting targeting vector was transfected into 129S3 mouse embryonic stem (ES) cells by electroporation. Neomycin resistant ES cell colonies were screened by polymerase chain reaction for homologous recombination. Correct targeting was confirmed by Southern blot using a neomycin-specific probe that allowed for the exclusion of random integration events

of the targeting vector. Selected targeted ES cells were injected into C57Bl/6 blastocysts and chimeric mice were bred with C57Bl/6 females, resulting in heterozygous *R899X* offspring that were back-crossed to C57Bl/6 for >5 generations.

Cardiopulmonary phenotyping, tissue collection and BMP9 treatment in mice

Three or six month-old mice were mice were anaesthetized with xylazine (4.6 mg/kg) and ketamine (7 mg/kg) and right and left ventricular pressures and volumes were recorded using a Millar PVR-1045 catheter (Millar Instruments, Houston, TX). Mice were then sacrificed and the hearts and lungs were harvested. Right ventricular hypertrophy was determined as a ratio of right ventricular to left ventricular and septal weight (RV/LV+S). The right lung was snap frozen in liquid nitrogen. The left lung was inflated with a 1:1 mixture of saline and OCT (Sakura, Zoeterwoude, Netherlands) and fixed with 4% paraformaldehyde in PBS prior to dehydration and paraffin embedding. A separate group of six month-old *Bmpr2+/R899X* mice and WT littermate controls were given daily i.p. injections of recombinant human BMP9 (75 ng/mouse/day, gift from Pfizer) for 28 days prior to evaluation of cardiopulmonary haemodynamics.

Monocrotaline rat model

Male Sprague Dawley rats (~200 to 250 grams, Charles River, Margate, UK) were randomized into three groups. Control rats were given intraperitoneal injections of sterile water as a vehicle control. Rats on the prevention protocol were given 60 mg/kg of MCT (Sigma, St. Louis, MO) by i.p. injection and treated with daily i.p. injections of recombinant human BMP9 (600 ng/day) or vehicle control from day 0 until sacrifice on days 2, 5 or 21. Rats on the reversal protocol were given 40 mg/kg of MCT, allowed to develop PAH from days 0 to 21, and treated with BMP9 (600 ng/day) or vehicle control from day 21 to sacrifice on day 35. At the time of sacrifice, animals were anaesthetized with xylazine (4.6 mg/kg) and ketamine (7 mg/kg) and right and left ventricular function were assessed using a Millar SPR-869 pressure-volume catheter. Tissue harvesting was carried out as described above for mice.

SU-5416-chronic hypoxia rat model

Male Sprague Dawley rats (~150 to 200 grams, Charles River) were given a single intraperitoneal injection of SU-5416 (20 mg/kg, Tocris, Bristol, UK) in vehicle (0.5% carboxyl methylcellulose sodium, 0.4% polysorbate 80, 0.9% Benzyl alcohol, all Sigma), placed immediately into a 10% O_2 chamber and maintained in hypoxia for 3 weeks, followed by 5 weeks in a normoxic environment to develop pulmonary hypertension. At the 8-week time point, rats were randomized into 3 groups. One group was assessed for cardiopulmonary function and sacrificed as described for the monocrotaline model above, while the other two groups received 3 weeks of daily i.p. injections with 600 ng/day BMP9 or saline vehicle as a control prior to cardiopulmonary phenotyping and sacrifice as described above.

SU-5416-chronic hypoxia mouse model

Six month-old male C57/BL6 mice (~30–35 g, Charles River) were given weekly subcutaneous (infrascapular) injections of SU-5416 (20 mg/kg) in vehicle (0.5% carboxyl methylcellulose sodium, 0.4% polysorbate 80, 0.9% Benzyl alcohol, all Sigma), placed immediately into a 10% O_2 chamber and maintained in hypoxia for 3 weeks. During this treatment period, mice were randomized into 4 groups. One group received vehicle alone without hypoxia or SU-5416, while another group received BMP9 (75 ng/day in saline i.p.) daily injections without hypoxia or SU-5416. Among mice receiving hypoxia and SU-5416, one group received vehicle while the remainder received BMP9 daily injections. In addition, a cohort of mice maintained in normoxia received daily intramuscular injections of BMP9 (75 ng/day) into the right hamstring muscle. Mice were assessed for cardiopulmonary function and sacrificed as described for the genetic mouse model above, and then subjected to conventional x-ray (Carestream in vivo imager) and micro-CT analysis (ScanCo μCT40).

Assessment of Nonsense Mediated Decay

PASMCs were seeded in 6cm plates and grown to approximately 1×10^3 cells/plate. Puromycin (Sigma) was added to 100 μg/ml for 20 h prior to harvesting. Parallel plates with and without puromycin were harvested for RNA analysis and a third plate for DNA. DNA was extracted using the QIAamp DNA Mini Kit (Qiagen, Valencia, CA) and RNA using the miRNeasy Mini Kit with on-column DNase treatment. First-strand cDNA synthesis was performed using Superscript III (Life Technologies, Carlsbad, CA) with random hexamer priming. The region of *BMPR2* exon 12 containing the *R899X* mutation was analyzed by dideoxy sequencing of PCR products (conditions and primers available on request). To ensure specificity for the target nucleic acid, DNA was amplified using an intronic reverse primer and RNA was amplified with primers spanning intron 12.

Immunohistochemistry

For assessment of pulmonary arteriolar muscularization, sections of fixed rat lung tissue (5μm) were labeled with monoclonal mouse-anti-mouse/rat/human smooth muscle α-actin (clone 1A4, Dako, Glostrup, Denmark), followed by polyclonal goat anti-mouse HRP. For mouse lung tissue, Dako ARK™ was used in accordance with the manufacturer's instructions. Briefly, the primary antibody was labeled by a modified biotinylated anti-mouse immunoblobulin prior to application to the specimen. The primary antibody and Biotinylation Reagent were mixed in solution, resulting in binding of biotinylated secondary antibody to the primary antibody. The Blocking Reagent, containing normal mouse serum, was then added to the mixture to bind residual Biotinylation Reagent not bound to the primary antibody, minimizing potential interaction with immunoglobulin endogenous in the specimen. The biotin-labeled primary antibody was then applied to the specimen followed by incubation with streptavidin-peoxidase and reaction with diaminobenzidine (DAB)/ hydrogen peroxide as substrate-chromogen.

Assessment of pulmonary arteriolar muscularization involved the identification of alveolar ducts and the subsequent categorization of the accompanying intra-acinar artery as non, partially or fully muscularized. A minimum of 20 vessels with diameters ranging from 25 to 75 μm were counted from non-serial lung sections and categorized as either fully, partially

or non-muscularized. Statistical significance was assessed by comparing the percentage of fully muscularized vessels between groups. Assesment of muscularization was performed blinded.

Alternatively, immunofluorescent assessment of mouse lung sections was performed using rabbit anti-vWF (Dako A0082) at 1:200 in 5% goat serum, followed by Alexa-488 conjugated anti-rabbit secondary antibody (Molecular Probes), as well as monoclonal anti-SM alpha actin (Sigma) at 1:100 in 5% goat serum followed by Alexa-555 conjugated anti-mouse secondary antibody (Molecular Probes).

For assessment of neointima formation, rat lung sections were also stained with Elastic Van Gieson (EVG) stain and examined by light microscopy. Quantification of endothelial cell apoptosis in rat lungs was performed by staining fixed rat lung sections with a rabbit monoclonal antibody towards cleaved caspase-3 (clone 5A1E, Cell Signaling Technology) or a rabbit polyclonal antibody towards vonWillebrand factor (catalogue # ab9378, Abcam, Cambridge, UK) and labeled using immunoperoxidase (Vectastain Elite, Vector Laboratories) and 3,3′-DAB to create a brown coloured reaction product. Cleaved caspase-3 positive cells on the luminal surface of 25 to 75 μm pulmonary vessels were vascular were quantified and normalized to total tissue area using Image J.

Ex-vivo stimulation of rat pulmonary artery and subsequent staining for phosphorylated Smad1/5 was performed as described previously for rat aortas[51]. Isolated pulmonary arteries were stimulated ex vivo for 1 hour with 5 ng/mL BMP9 prior to fixation and paraffin embedding.

Evans Blue Dye Permeability Assay

Permeability of Evans blue dye in response to LPS challenge was determined as described previously[52]. Briefly, animals were injected i.p. with 2mg/kg LPS (Sigma Aldrich) or vehicle and either 36.79 ng/25g recombinant human BMP9 or vehicle 22 hours prior to the i.p. injection of 6 mL/kg of 1% Evans blue dye in PBS with 4% bovine serum albumin (equivalent to 20 mg/kg Evans blue). Two hours after the injection of Evans blue, animals were sacrificed, the left atrium was clipped and the lung vasculature was flushed with 10mL of PBS per mouse via the right ventricle to remove intravascular EB. Flushed lungs were photographed and right and left lungs were separately weighted and snap frozen in liquid nitrogen. Right lungs were homogenized in formamide (1ml/100mg lung), and incubated for 24 hr at 37°C. Homogenates were clarified by centrifugation at 12,000 g for 20 min and the absorbance of 200μl of clarified supernatant was measured at 620nm in a 96-well plate.

Statistical Methods

Student's t-tests were used for comparisons between two groups. Multiple comparisons were assessed by one-way ANOVA, followed by the appropriate post-hoc test for significance, as specified in the figure legends. Equivalence of variance between experimental groups was confirmed using an F-test for comparisons between two groups and a Brown-Forsythe test in conjunction with ANOVA, when applicable. Normal distribution was assumed for all statistical analyses and confirmed when group sizes allowed for testing of normality. All statistical tests used two-sided tests of significance. All data are reported as mean +/− SEM.

Supplementary Material

Refer to Web version on PubMed Central for supplementary material.

Acknowledgments

References

1. Morrell NW, et al. Cellular and molecular basis of pulmonary arterial hypertension. J Am Coll Cardiol. 2009; 54:S20–31. [PubMed: 19555855]

2. Gaine SP, Rubin LJ. Primary pulmonary hypertension. Lancet. 1998; 352:719–725. [PubMed: 9729004]

3. Lane KB, et al. Heterozygous germline mutations in BMPR2, encoding a TGF-beta receptor, cause familial primary pulmonary hypertension. The International PPH Consortium. Nat Genet. 2000; 26:81–84. [PubMed: 10973254]

4. Deng Z, et al. Familial primary pulmonary hypertension (gene PPH1) is caused by mutations in the bone morphogenetic protein receptor-II gene. Am J Hum Genet. 2000; 67:737–744. [PubMed: 10903931]

5. Thomson JR, et al. Sporadic primary pulmonary hypertension is associated with germline mutations of the gene encoding BMPR-II, a receptor member of the TGF-beta family. J Med Genet. 2000; 37:741–745. [PubMed: 11015450]

6. Atkinson C, et al. Primary pulmonary hypertension is associated with reduced pulmonary vascular expression of type II bone morphogenetic protein receptor. Circulation. 2002; 105:1672–1678. [PubMed: 11940546]

7. Long L, et al. Altered bone morphogenetic protein and transforming growth factor-beta signaling in rat models of pulmonary hypertension: potential for activin receptor-like kinase-5 inhibition in prevention and progression of disease. Circulation. 2009; 119:566–576. [PubMed: 19153267]

8. Hong KH, et al. Genetic ablation of the BMPR2 gene in pulmonary endothelium is sufficient to predispose to pulmonary arterial hypertension. Circulation. 2008; 118:722–730. [PubMed: 18663089]

9. Reynolds AM, Holmes MD, Danilov SM, Reynolds PN. Targeted gene delivery of BMPR2 attenuates pulmonary hypertension. Eur Respir J. 2012; 39:329–343. [PubMed: 21737550]

10. Reynolds AM, et al. Bone morphogenetic protein type 2 receptor gene therapy attenuates hypoxic pulmonary hypertension. Am J Physiol Lung Cell Mol Physiol. 2007; 292:L1182–1192. [PubMed: 17277049]

11. Spiekerkoetter E, et al. FK506 activates BMPR2, rescues endothelial dysfunction, and reverses pulmonary hypertension. J Clin Invest. 2013; 123:3600–3613. [PubMed: 23867624]

12. Trembath RC, et al. Clinical and molecular genetic features of pulmonary hypertension in patients with hereditary hemorrhagic telangiectasia. N Engl J Med. 2001; 345:325–334. [PubMed: 11484689]

13. Harrison RE, et al. Molecular and functional analysis identifies ALK-1 as the predominant cause of pulmonary hypertension related to hereditary haemorrhagic telangiectasia. J Med Genet. 2003; 40:865–871. [PubMed: 14684682]

14. Yeager ME, Halley GR, Golpon HA, Voelkel NF, Tuder RM. Microsatellite instability of endothelial cell growth and apoptosis genes within plexiform lesions in primary pulmonary hypertension. Circ Res. 2001; 88:E2–E11. [PubMed: 11139485]

15. Teichert-Kuliszewska K, et al. Bone morphogenetic protein receptor-2 signaling promotes pulmonary arterial endothelial cell survival: implications for loss-of-function mutations in the pathogenesis of pulmonary hypertension. Circ Res. 2006; 98:209–217. [PubMed: 16357305]

16. Wilson DW, et al. Mechanisms and pathology of monocrotaline pulmonary toxicity. Crit Rev Toxicol. 1992; 22:307–325. [PubMed: 1489509]

17. Taraseviciene-Stewart L, et al. Inhibition of the VEGF receptor 2 combined with chronic hypoxia causes cell death-dependent pulmonary endothelial cell proliferation and severe pulmonary hypertension. Faseb J. 2001; 15:427–438. [PubMed: 11156958]

18. Burton VJ, et al. Bone morphogenetic protein receptor II regulates pulmonary artery endothelial cell barrier function. Blood. 2011; 117:333–341. [PubMed: 20724539]

19. Burton VJ, et al. Attenuation of leukocyte recruitment via CXCR1/2 inhibition stops the progression of PAH in mice with genetic ablation of endothelial BMPR-II. Blood. 2011; 118:4750–4758. [PubMed: 21900197]

20. Kim CW, et al. Anti-Inflammatory and Antiatherogenic Role of BMP Receptor II in Endothelial Cells. Arterioscler Thromb Vasc Biol. 2013; 33:1350–1359. [PubMed: 23559633]

21. Yang J, et al. Mutations in bone morphogenetic protein type II receptor cause dysregulation of Id gene expression in pulmonary artery smooth muscle cells: implications for familial pulmonary arterial hypertension. Circ Res. 2008; 102:1212–1221. [PubMed: 18436795]

22. Miyazono K, Maeda S, Imamura T. BMP receptor signaling: transcriptional targets, regulation of signals, and signaling cross-talk. Cytokine Growth Factor Rev. 2005; 16:251–263. [PubMed: 15871923]

23. David L, Mallet C, Mazerbourg S, Feige JJ, Bailly S. Identification of BMP9 and BMP10 as functional activators of the orphan activin receptor-like kinase 1 (ALK1) in endothelial cells. Blood. 2007; 109:1953–1961. [PubMed: 17068149]

24. Scharpfenecker M, et al. BMP-9 signals via ALK1 and inhibits bFGF-induced endothelial cell proliferation and VEGF-stimulated angiogenesis. J Cell Sci. 2007; 120:964–972. [PubMed: 17311849]

25. David L, et al. Bone morphogenetic protein-9 is a circulating vascular quiescence factor. Circ Res. 2008; 102:914–922. [PubMed: 18309101]

26. Frank DB, et al. Increased susceptibility to hypoxic pulmonary hypertension in Bmpr2 mutant mice is associated with endothelial dysfunction in the pulmonary vasculature. Am J Physiol Lung Cell Mol Physiol. 2008; 294:L98–109. [PubMed: 18024717]

27. Song Y, et al. Increased susceptibility to pulmonary hypertension in heterozygous BMPR2-mutant mice. Circulation. 2005; 112:553–562. [PubMed: 16027259]

28. Kang Q, et al. Characterization of the distinct orthotopic bone-forming activity of 14 BMPs using recombinant adenovirus-mediated gene delivery. Gene therapy. 2004; 11:1312–1320. [PubMed: 15269709]

29. Slowik MR, et al. Evidence that tumor necrosis factor triggers apoptosis in human endothelial cells by interleukin-1-converting enzyme-like protease-dependent and -independent pathways. Lab Invest. 1997; 77:257–267. [PubMed: 9314949]

30. Upton PD, Davies RJ, Trembath RC, Morrell NW. Bone morphogenetic protein (BMP) and activin type II receptors balance BMP9 signals mediated by activin receptor-like kinase-1 in human pulmonary artery endothelial cells. J Biol Chem. 2009; 284:15794–15804. [PubMed: 19366699]

31. Beppu H, et al. BMP type II receptor is required for gastrulation and early development of mouse embryos. Dev Biol. 2000; 221:249–258. [PubMed: 10772805]

32. Machado RD, et al. Mutations of the TGF-beta type II receptor BMPR2 in pulmonary arterial hypertension. Hum Mutat. 2006; 27:121–132. [PubMed: 16429395]

33. Lechleider RJ, et al. Targeted mutagenesis of Smad1 reveals an essential role in chorioallantoic fusion. Dev Biol. 2001; 240:157–167. [PubMed: 11784053]

34. Reynolds AM, Holmes MD, Danilov SM, Reynolds PN. Targeted gene delivery of BMPR-2 attenuates pulmonary hypertension. Eur Respir J. 2011

35. Valdimarsdottir G, et al. Stimulation of Id1 expression by bone morphogenetic protein is sufficient and necessary for bone morphogenetic protein-induced activation of endothelial cells. Circulation. 2002; 106:2263–2270. [PubMed: 12390958]

36. Ciumas M, et al. Bone Morphogenetic Proteins Protect Pulmonary Microvascular Endothelial Cells From Apoptosis by Upregulating alpha-B-Crystallin. Arterioscler Thromb Vasc Biol. 2013; 33:2577–2584. [PubMed: 24072698]

37. Prewitt AR, et al. Heterozygous null bone morphogenetic protein receptor type 2 mutations promote SRC kinase-dependent caveolar trafficking defects and endothelial dysfunction in pulmonary arterial hypertension. J Biol Chem. 2015; 290:960–971. [PubMed: 25411245]

38. Nasim MT, et al. Molecular genetic characterization of SMAD signaling molecules in pulmonary arterial hypertension. Hum Mutat. 2011; 32:1385–1389. [PubMed: 21898662]

39. Drake KM, et al. Altered MicroRNA processing in heritable pulmonary arterial hypertension: an important role for Smad-8. Am J Respir Crit Care Med. 2011; 184:1400–1408. [PubMed: 21920918]

40. Han C, et al. SMAD1 deficiency in either endothelial or smooth muscle cells can predispose mice to pulmonary hypertension. Hypertension. 2013; 61:1044–1052. [PubMed: 23478097]

41. Hemnes AR, et al. Evidence for Right Ventricular Lipotoxicity in Heritable Pulmonary Arterial Hypertension. Am J Respir Crit Care Med. 2013

42. Geti I, et al. A Practical and Efficient Cellular Substrate for the Generation of Induced Pluripotent Stem Cells from Adults: Blood-Derived Endothelial Progenitor Cells. Stem Cells Translational Medicine. 2012; 1:855–865. [PubMed: 23283547]

43. Allport JR, et al. Neutrophils from MMP-9- or neutrophil elastase-deficient mice show no defect in transendothelial migration under flow in vitro. J Leukoc Biol. 2002; 71:821–828. [PubMed: 11994507]

44. Yang X, et al. Dysfunctional Smad signaling contributes to abnormal smooth muscle cell proliferation in familial pulmonary arterial hypertension. Circ Res. 2005; 96:1053–1063. [PubMed: 15845886]

45. Smyth, GK. Limma: linear models for microarray data. In: Gentleman, R.; Carey, V.; Dudoit, S.; Irizarry, R.; WH, editors. Bioinformatics and Computational Biology Solutions using R and Bioconductor. Springer; New York: 2005. p. 397-420.

46. Luo W, Friedman MS, Shedden K, Hankenson KD, Woolf PJ. GAGE: generally applicable gene set enrichment for pathway analysis. BMC bioinformatics. 2009; 10:161. [PubMed: 19473525]

47. Tarca AL, et al. A Novel Signaling Pathway Impact Analysis (SPIA). Bioinformatics. 2008

48. Luo W, Brouwer C. Pathview: an R/Bioconductor package for pathway-based data integration and visualization. Bioinformatics. 2013; 29:1830–1831. [PubMed: 23740750]

49. Harrington EO, et al. Role of protein kinase C isoforms in rat epididymal microvascular endothelial barrier function. Am J Respir Cell Mol Biol. 2003; 28:626–636. [PubMed: 12707019]

50. Waters JP, et al. In vitro self-assembly of human pericyte-supported endothelial microvessels in three-dimensional coculture: a simple model for interrogating endothelial-pericyte interactions. J Vasc Res. 2013; 50:324–331. [PubMed: 23860328]

51. Bidart M, et al. BMP9 is produced by hepatocytes and circulates mainly in an active mature form complexed to its prodomain. Cellular and molecular life sciences: CMLS. 2012; 69:313–324. [PubMed: 21710321]

52. Moitra J, Sammani S, Garcia JG. Re-evaluation of Evans Blue dye as a marker of albumin clearance in murine models of acute lung injury. Translational research: the journal of laboratory and clinical medicine. 2007; 150:253–265. [PubMed: 17900513]
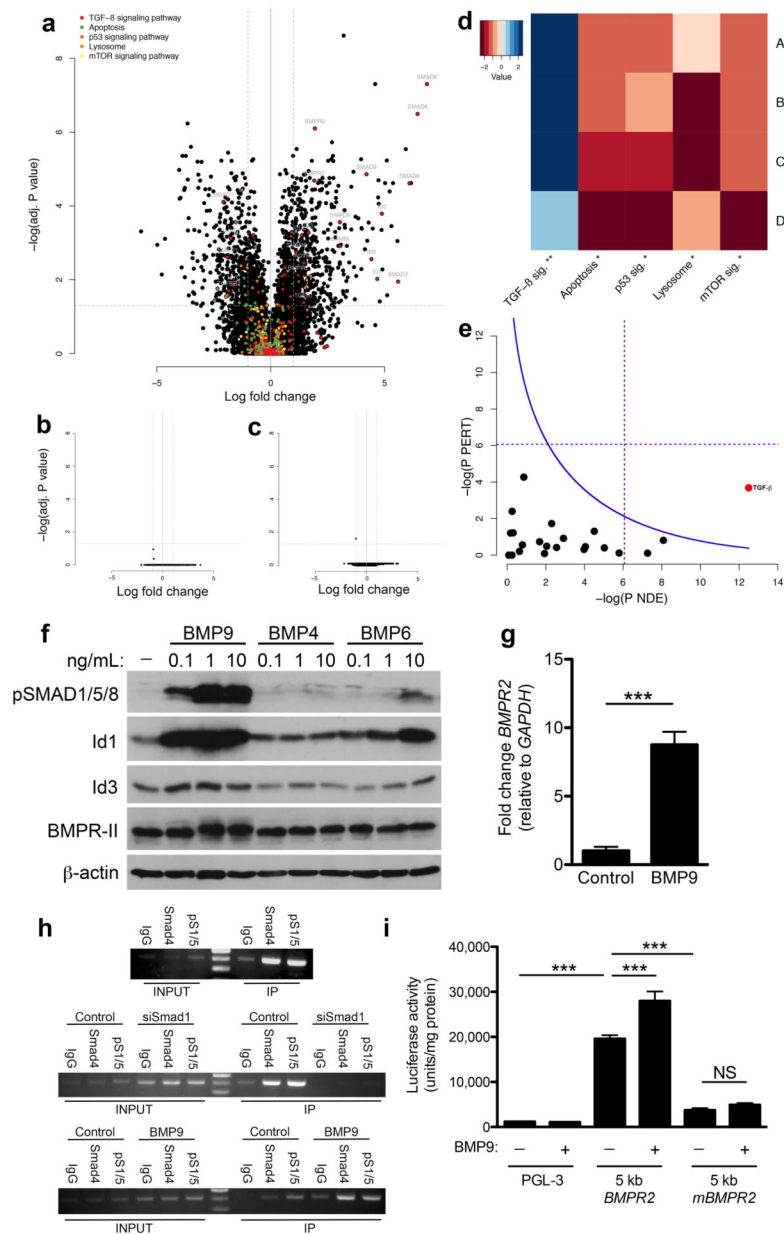
Figure 1. BMP9 preferentially stimulates hPAECs

Volcano plots of differentially expressed genes in PAECs treated with (**a**) 1 ng/mL BMP9, (**b**) 10 ng/mL BMP6 or (**c**) 10 ng/mL BMP2 versus control after fitting linear models and adjusting P values for multiple testing (FDR). Differentially expressed genes of the TGF-β pathway are highlighted in grey. Dashed lines represent an adjusted P value of 0.05 and a fold change of +/− 1x. (**d**) Heat map showing whole gene-set perturbation (test statistics) of regulated pathways in PAECs following BMP9 treatment. (**e**) Signaling pathway impact analysis (SPIA) to detect alterations in common signaling pathways in PAECs in response to BMP9 treatment. Corrected for false discovery rate. (**f**) Immunoblotting for phosphorylated Smad1/5/8, Id1, Id3, BMPR-II and β-actin in PAECs cultured with or without varying concentrations of BMP9, BMP4 and BMP6 ligand for 2 hours. Representative of 3

experiments. (**g**) Expression of *BMPR2* in PAECs with or without treatment with 10 ng/mL BMP9 for 24 hours (n=3; Student's t test). (**h**) Representative agarose gels for products from chromatin immunoprecipitation on lysates from HMEC-1 cells (top) without treatment, (middle) 72 hours after siRNA knockdown of SMAD1 or (bottom) following a 24 hour treatment with 1 ng/mL BMP9. (**i**) Luciferase activity in HMEC-1 lysates transfected with a luciferase reporter construct with or without an upstream 5kb portion of the *BMPR2* promoter with or without mutation of the putative Smad binding region. Cells bearing the reporter construct were treated with 10 ng/mL BMP9 for 24 hours (n=3; 1-way ANOVA, Tukey's post test). ***P<0.001, **P<0.01, *P<0.05. Mean +/− SEM.
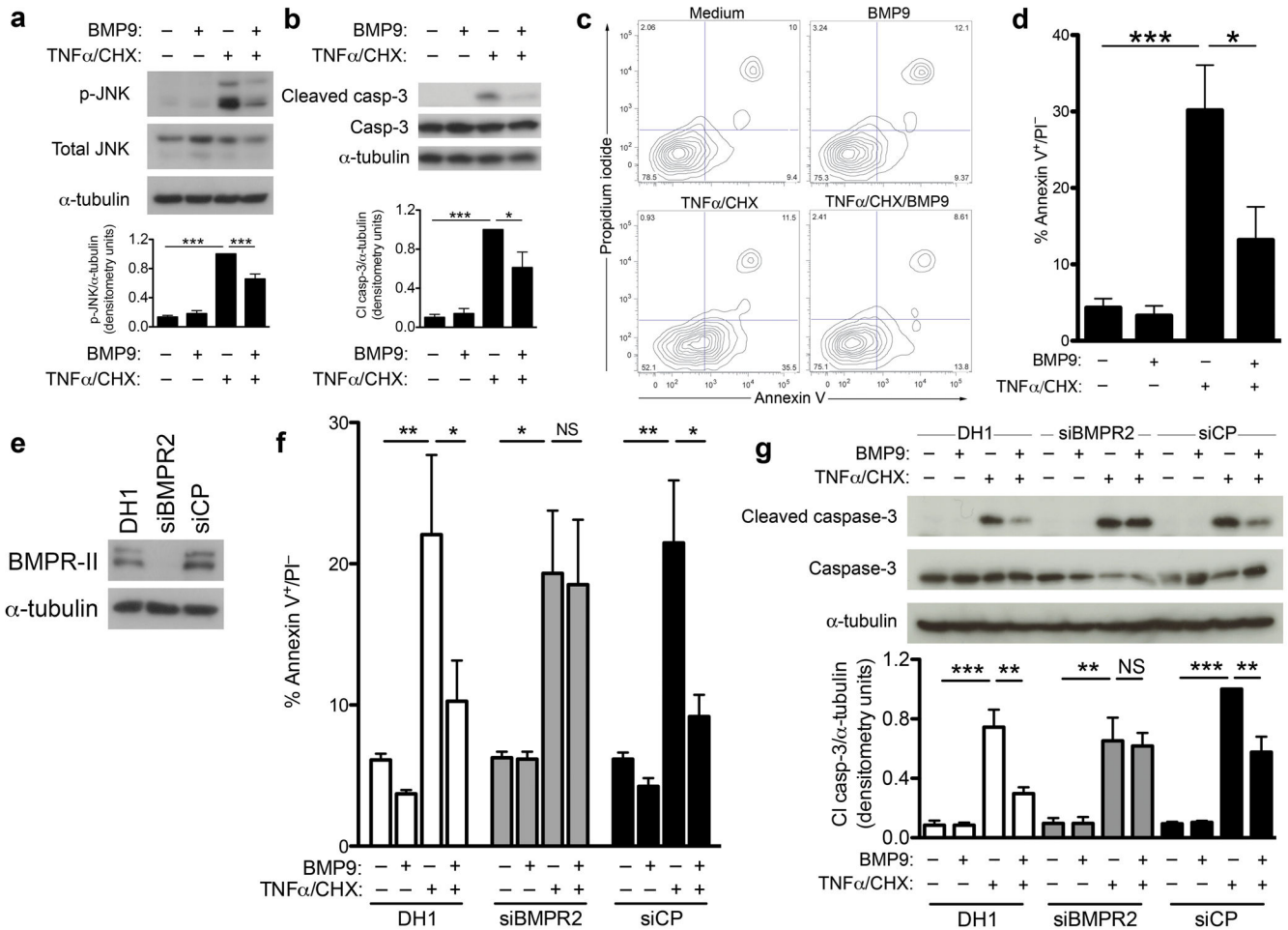
**Figure 2. BMP9 prevents apoptosis in human PAECs via BMPR-II**

Representative immunoblots and densitometric analysis for (**a**) phosphorylated JNK (n=4) and (**b**) cleaved caspase 3 (n=3) in human PAECs cultured with or without BMP9 (5 ng/mL) for 16 hours prior to an apoptotic stimulus with TNFα (10 ng/mL) and cyclohexamide (20 μg/mL) (1-way ANOVA, Tukey's post test). (**c**) Representative flow cytometry plots of human PAECs stained with Annexin-V and propidium iodide (PI) with or without BMP9 pre-treatment and apoptotic stimulus. (**d**) Quantification of apoptotic (Annexin-V$^+$/PI$^-$) PAECs (n=5); 1-way ANOVA, Tukey's post test). (**e**) Validation of siRNA knockdown in PAECs by immunoblotting for BMPR-II following treatment with either Dharmafect 1 transfection reagent (DH1), siRNA for *BMPR2* (siBMPR2) or a pooled siRNA control (siCP). (**f**) Cytometric quantification of apoptosis by staining for Annexin-V and PI in PAECs treated with DH1 alone, siBMPR2 or siCP and cultured with or without BMP9 pre-treatment and apoptotic stimulus (n=6 for DH1 and siBMPR-II, n=5 for siCP; 1-way ANOVA for each siRNA group, Tukey's post test). (**g**) Representative immunoblot and densitometric analysis of cleaved caspase-3 in PAECs following siRNA transfection with or without BMP9 pre-treatment and apoptotic stimulus. (n=3; 1-way ANOVA for each siRNA group, Tukey's post test). All blots were re-probed for α-tubulin as a loading control. ***P<0.001, **P<0.01, * P<0.05. Mean +/− SEM.
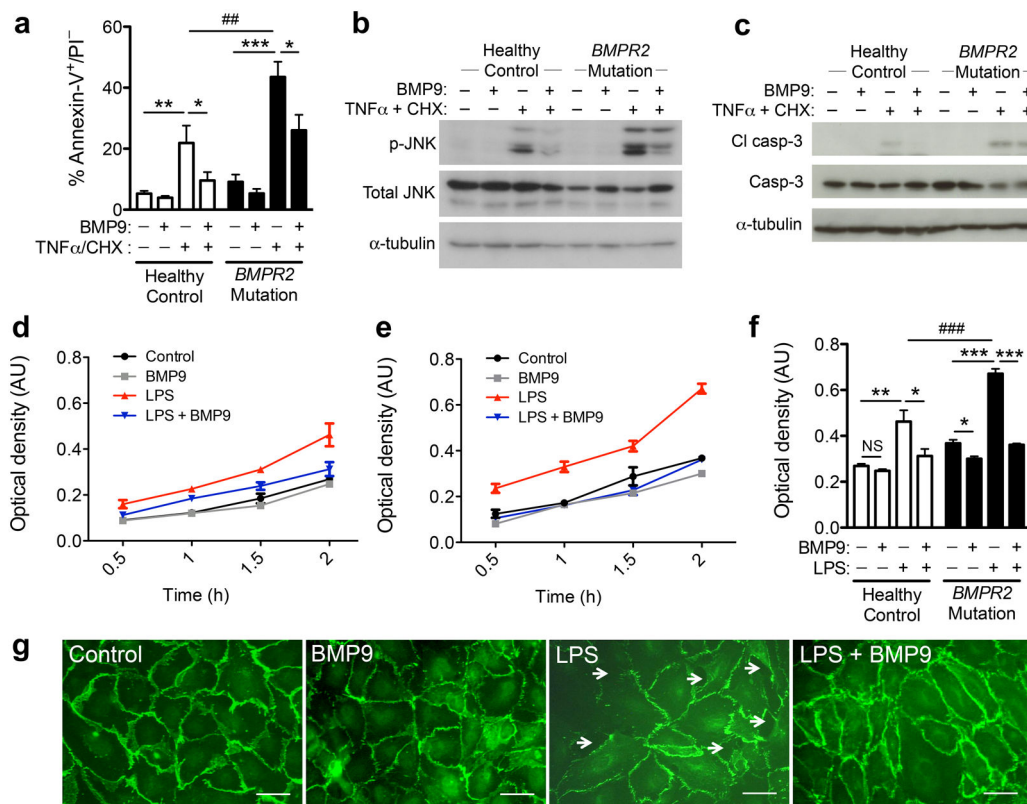
**Figure 3. BMP9 prevents apoptosis and promotes monolayer integrity in BOECs with and without BMPR-II mutations**

(**a**) Quantification of apoptotic (Annexin-V$^+$/PI$^-$) control (n=5 individuals) and *BMPR2* mutation-bearing BOECs (n=6 individuals) after culture with or without BMP9 (5 ng/mL) for 16 hours prior to the addition of TNFα (10 ng/mL) and cyclohexamide (20 µg/mL) for 6 hours. (**b–c**) Immunoblotting for (**b**) phosphorylated JNK and (**c**) cleaved caspase-3 in control and *BMPR2* mutation-bearing BOECs with or without BMP9 pre-treatment and apoptotic stimulus. Representative of five immunoblots. All blots were re-probed for α-tubulin as a loading control. (**d–f**) Permeability of (**d**) control or (**e**) *BMPR2* mutation-bearing BOEC monolayers to HRP, assessed as a measure of colorimetric absorbance after incubation periods ranging from 30 minutes to 2 hours with or without BMP9 (20 ng/mL) and/or LPS (400 ng/mL) (**f**) Quantification of monolayer permeability at 2 hours post-LPS. (n=4 individuals per group). AU: Arbitraty units. ***P<0.001, **P<0.01, *P<0.05, 1-way ANOVA, repeated measures Tukey's post test for Control or *BMPR2* Mutation BOECs; ###P<0.001, ##P<0.01, 1-way ANOVA, Tukey's post test for all groups. Mean +/− SEM. (**g**) Representative immunofluorescence images of PAECs stained for VE-cadherin following 24 hour culture with or without BMP9 (10 ng/mL) and/or LPS (400 ng/mL). Scale bars 10 µm.
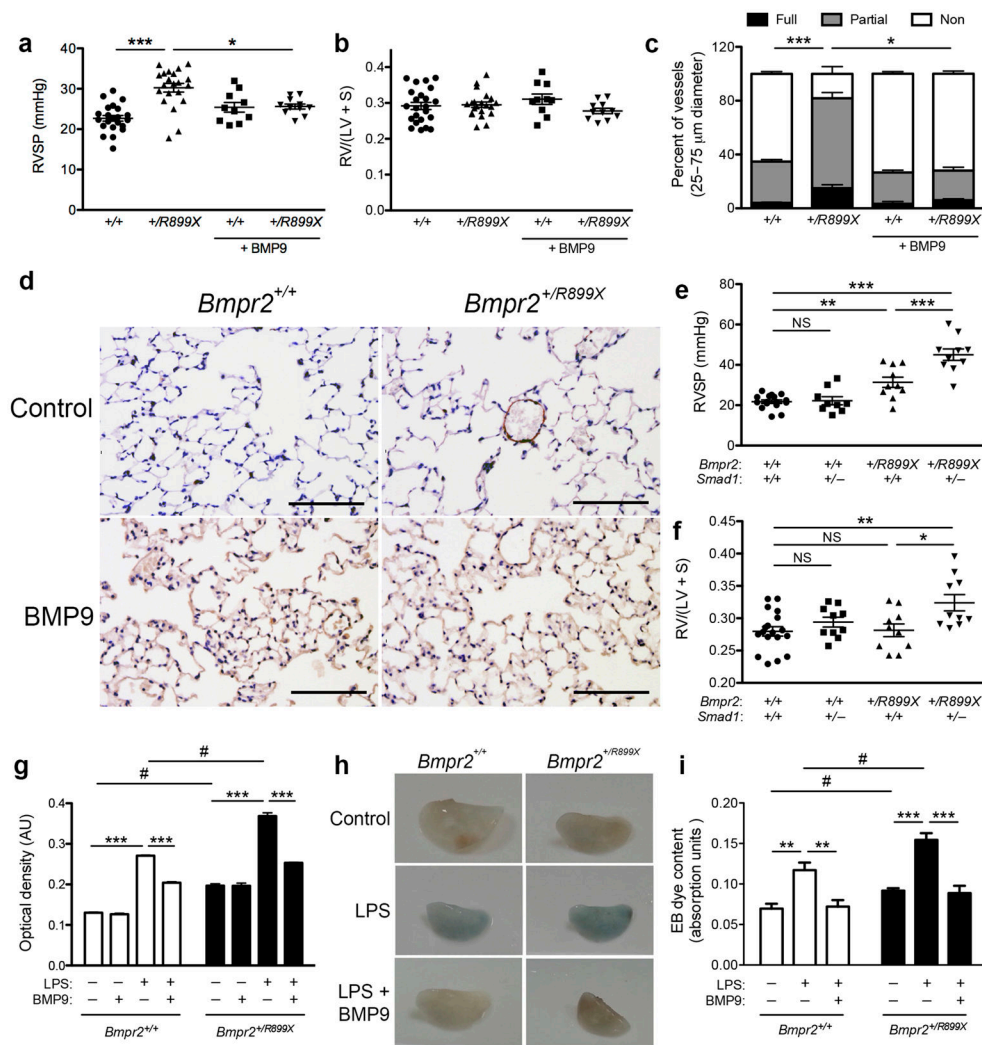
Figure 4. Pulmonary hypertension in *Bmpr2^{+/R899X}* knock-in mice is reversed by BMP9
(**a**) Assessment of right ventricular systolic pressure (RVSP) in 6-month-old, naive
Bmpr2^{+/R899X} mice (n=21, 11 male, 10 female) and WT littermate controls (n=23, 13 male,
10 female) or with 4 weeks of BMP9 treatment (75 ng/day, i.p., n=10 (9 male, 1 female) for
WT and n=11 (9 male, 2 female) for *Bmpr2^{+/R899X}*; 1-way ANOVA, Tukey's post test). (**b**)
Right ventricular hypertrophy (Fulton index, ratio of RV weight over LV and septal weight)
in the same animals as **a** (not significant). (**c**) Quantitative assessment of pulmonary arterial
muscularization in the same groups as **a**. Displayed as a non-, partially- and fully-
muscularized arteries as a percentage of total alveolar wall and duct arteries (n=12 (6 male,
6 female) for naïve WT and *Bmpr2^{+/R899X}* mice; with BMP9 treatment n=3 (2 male, 1
female) for WT and n=5 (3 male, 2 female) for *Bmpr2^{+/R899X}*; 1-way ANOVA, Tukey's
post test). (**d**) Representative images of immunohistochemical staining for smooth muscle α-
actin in lung sections from WT and *Bmpr2^{+/R899X}* mice with or without BMP9 treatment. (**e**)
Assessment of RVSP and (**f**) RV hypertrophy in male 6 month-old WT (n=16), *Smad1^{+/−}*
(n=9), *Bmpr2^{+/R899X}* (n=10) and compound *Bmpr2^{+/R899X}/Smad1^{+/−}* heterozygotes (n=10;
1-way ANOVA, Tukey's post test). (**g**) Quantification of monolayer permeability at 2 hours

post-LPS. (n=3; 1-way ANOVA, repeated measures Tukey's post test for WT or *Bmpr2*[+/*R899X*] cells; #P<0.05, 1-way ANOVA, Tukey's post test for all groups). AU: Arbitrary units. (**h**) Images of lungs isolated from mice injected with 2 mg/kg LPS or vehicle and either 36.79 ng/25g BMP9 or vehicle (all i.p.) 22 hours prior to the i.p. injection of Evans blue dye, which was delivered 2 hours prior to sacrifice. (**i**) Quantitative assessment of extravascular Evans blue dye in the lungs of the mice described in **h** (Control: n=7 (5 male, 2 female) for WT, n=9 (4 male, 5 female) for *Bmpr2*[+/*R899X*]; LPS: n=8 (5 male, 3 female) for WT, n=10 (6 male, 4 female) for *Bmpr2*[+/*R899X*]; LPS + BMP9: n=8 (4 male, 4 female) for WT, n=9 (5 male, 4 female) for *Bmpr2*[+/*R899X*]; 1-way ANOVA, Tukey's post test for WT or *Bmpr2*[+/*R899X*] mice; #P<0.05, 1-way ANOVA, Tukey's post test for all groups). ***P<0.001, **P<0.01, *P<0.05. Mean +/− SEM.
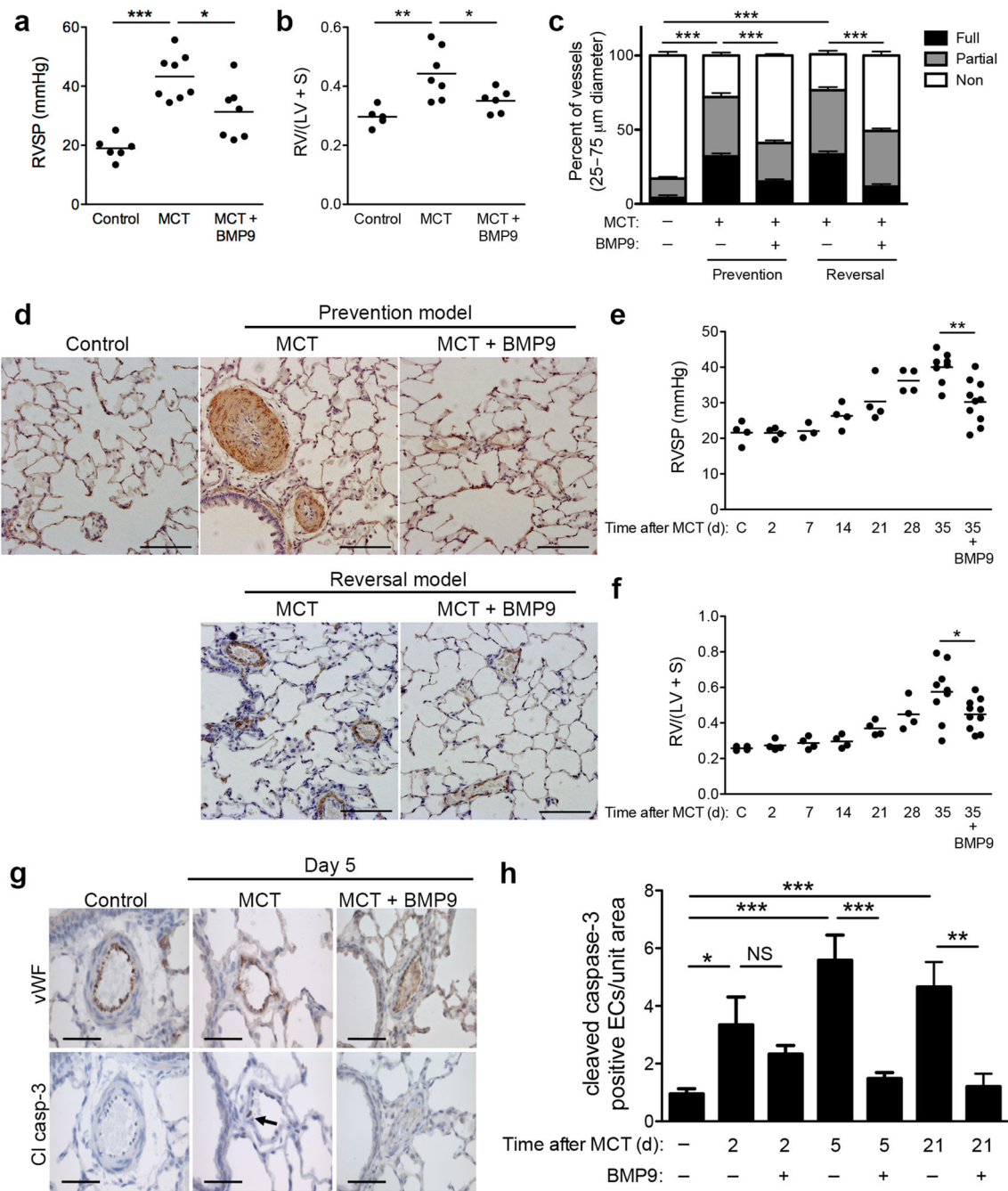
Figure 5. BMP9 reverses established monocrotaline-induced pulmonary hypertension and prevents endothelial cell apoptosis in rats

(**a**) Assessment of right ventricular systolic pressure (RVSP) and (**b**) RV hypertrophy (Fulton index) in rats on a prevention protocol given vehicle (n=6) or monocrotaline (60 mg/kg, i.p.) and treated with BMP9 (n=7, 600 ng/day, i.p.) or vehicle (n=8) from days 0 to 21 post-MCT (1-way ANOVA, Tukey's post test). (**c**) Quantitative assessment of pulmonary arterial muscularization in control rats or rats given monocrotaline, followed by daily injections with saline or BMP9 in a prevention (days 0–21 post-MCT) or reversal (days 21–

35 post-MCT) protocol. Displayed as non-, partially- and fully-muscularized arteries as a percentage of total alveolar wall and duct arteries (n=5 for prevention, n=6 for reversal; 1-way ANOVA, Tukey's post test for fully muscularized vessels). (**d**) Immunohistochemical staining for smooth muscle α-actin in lung sections from the rats as described in **c**. Scale bars 100 μm. (**e**) Assessment of right ventricular systolic pressure (RVSP) and (**f**) RV hypertrophy (Fulton index) in rats on a reversal protocol given vehicle (n=4) or monocrotaline (40 mg/kg, i.p.) and treated with BMP9 (n=10, 600 ng/day) or vehicle (n=9) from days 21 to 35 post-MCT (t test on 35 day groups treated with saline or BMP9). (**g**) Representative images of immunohistochemical staining for von Willebrand Factor (upper) and cleaved caspase-3 (lower) in lung sections from rats given vehicle control or monocrotaline (60 mg/kg, i.p.), treated with BMP9 (600 ng/day, i.p.) or saline from day 0 and sacrificed on day 5 post-MCT. Scale bars 50 μm. (**h**) Quantification of cleaved caspase-3 positive endothelial cells in lung sections from the groups described in **a**, **b** and **g** and sacrificed on days 2, 5 or 21 post-MCT (n=11 for Control, n=6 for days 2 and 5 post-MCT, n=5 for day 21 post-MCT; 1-way ANOVA, Tukey's post test). ***$P<0.001$, **$P<0.01$, *$P<0.05$. Mean +/− SEM.
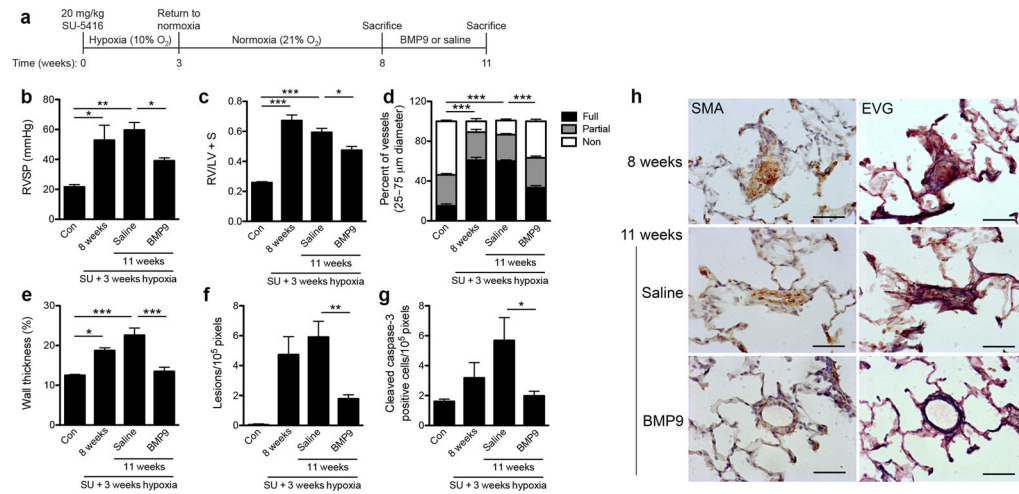
Figure 6. BMP9 reverses established pulmonary hypertension in rats in response to treatment with the VEGF receptor inhibitior SU-5416 in combination with chronic hypoxia
(**a**) Rats were given vehicle injections and maintained in normoxia (n=4) or challenged with SU-5416 (20 mg/kg, i.p.) and 3 weeks hypoxia (10% O$_2$) prior to 5 weeks normoxia and assessment at 8 weeks (n=7) or at 11 weeks following daily treatment with saline vehicle (n=11) or BMP9 (n=11; 600 ng/day, i.p.). (**b**) Assessment of right ventricular systolic pressure (RVSP) and (**c**) RV hypertrophy (Fulton index) for the rats described in **a** (1-way ANOVA, Tukey's post test). (**d**) Quantification of non-, partially- and fully-muscularized arteries as a percentage of total alveolar wall and duct arteries (n=4 for control, n=6 for all other groups; 1-way ANOVA, Tukey's post test for fully muscularized vessels). (**e**) Assessment of pulmonary arterial wall thickness as a percentage of luminal diameter (n=4 for control, n=6 for all other groups; 1-way ANOVA, Tukey's post test). (**f**) Quantification of neointimal lesion frequency in the lungs of the rats described in **a** (n=3 for control, n=6 for all other groups; 1-way ANOVA, Tukey's post test). (**g**) Quantification of cleaved caspase-3 positive endothelial cells in lung sections from the groups described in **a** (n=3 for control, n=6 for all other groups; 1-way ANOVA, Tukey's post test). ***P<0.001, **P<0.01, *P<0.05. Mean +/− SEM. (**h**) Neointima formation in the lungs of the rats described in **a**. Lung sections were stained for smooth muscle α-actin (SMA) or with elastic van Gieson (EVG) stain. Scale bar = 50μm.